# Axial Impact Collapse Analysis of Spot Welded Hat and Double-hat Shaped Section Members Using an Explicit Finite Element Code

**Cheon Seok Cha, Young Nam Kim**
*Department of Mechanical Design Engineering Graduate school, Chosun University*
**Sun Kyu Kim**
*Department of Automobile Engineering, Iksan National Collage*
**Kwang Hee Im**
*Department of Automotive Engineering, Woosuk University*
**In Young Yang**
*School of Mechanical Engineering, Chosun University*

The purpose of this study is to analyze the collapse characteristics of widely used spot welded section members (hat and double hat section members of vehicles) which possess the greatest energy absorbing capacity in an axial impact collapse. This study also suggests how the collapse load and deformation mode are obtained under impact. In the program system presented in this study, an explicit finite element code, LS-DYNA3D, is adopted for simulating complicated collapse behavior of the hat and double hat shaped section members with respect to section dimensions and spot weld pitches. Comparing the results with experiments, the simulation has been verified under a velocity of 7.19 m/sec (impact energy of 1034J).

**Key Words :** Spot Welded Section Members, Axial Impact Collapse, Deformation Mode, Collapse Characteristics, Simulation, Experiment

## 1. Introduction

The hat shaped section members of vehicles compose the base frame which plays an important role in a front-end collision. This consists of the hat shaped section members using spot welds. Even though this member is not closed in section, it is regarded as a closed box shaped member.

Studies of the collapse characteristics of spot welded section members are extended to theoretically analyze the mean collapse loads assuming it as perfectly seamless in section and to experimentally estimate the static mean collapse loads (White et al., 1999a; White et al., 1999b). With the breakthrough developments of computer and finite element methods, many researchers have used computers to predict the collapse characteristics (Yamaxaki et al, 1998; Santosa, 1998). However, it is very difficult to theoretically analyze impact behavior of the section members because they are not closed except for the area of the spot weld. And it is hard to find literature to define the optimal conditions on the shift of spot weld pitch and section dimension in the impact collapse.

The spot welded hat shaped section members of vehicles absorb most of the impact energy in a front-end collision. In this study, the specimens with various section dimensions and spot weld pitches on the flange have been tested with a high impact velocity (7.19 m/sec) which simulates an actual car crash. The energy absorbing capacity will be analyzed and an analysis method will be suggested to obtain exact collapse loads and deformation collapse modes. The material

* Corresponding Author,
**E-mail** : iyyang@mail.chosun.ac.kr
**TEL** : +82-62-230-7170; **FAX** : +82-62-230-7170
School of Mechanical Engineering, Chosun University, 375 Seosuk-dong, Dong-gu, Kwangju 501-759, Korea.
(Manuscript **Received** February 17, 2001; **Revised** October 12, 2001)

undergoes non-linear behavior and is dependent on the strain rate until it buckles. Considering the non-linearity in material being dependent on strain rate, impact collapse simulation has been carried out, on the same condition as in the experiment, to analyze unmeasurable and complex mechanisms: the deformation collapse modes and relationship between stress and deformation.

Using an explicit finite element code, LS-DYNA3D, the axial impact collapse simulation on the sections has been carried out. By doing the axial impact collapse experiments and comparing the experimental results (Cha et al., 2001) with those from the simulation, the simulation has been verified. The simulation can evaluate the structural capacity of various conditions and predict how effective a structural modification will be on the energy absorbing capacity before the actual modification is applied. Furthermore, it is helpful to save time consumption and financial cost. The axial collapse under impact has been studied, so the simulation enables us to accurately predict how the section would be affected by the interference and shapes which are unknown in experiments. It also provides the stress-strain distribution in the section. An analysis of the collapse mechanisms under impact is to understand the impact characteristics of structures, to acquire useful information for optimal design.

## 2. Specimens and Impact Collapse Experiment

### 2.1 Specimens

The specimens, hat and double hat shaped section members, were manufactured by welding two parts of SCP1, cold rolled sheet metal which is widely used for these structures. The specifications of specimens are shown in Table 1. All the specimens have a flange width of 12 mm. By doing several preliminary tests, the length of 120 mm was selected in order for Eulian buckling not to occur, and to obtain repetitive and agreeable experimental results. The hat and double hat shaped section members with thicknesses of 0.78 mm and 0.95 mm, section dimensions of 30×30 mm, 33×27 mm and 36×24 mm were selected.

**Table 1** Specifications of the specimens

| Name | Type | Thickness [mm] | Section dimensions b×h [mm×mm] | Section dimensions R=b/h | Spot weld pitch[mm] |
|---|---|---|---|---|---|
| H078WE | Hat | 0.78 | 30×30 | 1 | 18.3 |
| H078WF | Hat | 0.78 | 30×30 | 1 | 22 |
| H078WG | Hat | 0.78 | 30×30 | 1 | 27.5 |
| H078XF | Hat | 0.78 | 33×27 | 1.22 | 22 |
| H078YF | Hat | 0.78 | 36×24 | 1.5 | 22 |
| H095WF | Hat | 0.95 | 30×30 | 1 | 22 |
| H095XF | Hat | 0.95 | 33×27 | 1.22 | 22 |
| H095YF | Hat | 0.95 | 36×24 | 1.5 | 22 |
| D078WE | Double hat | 0.78 | 30×30 | 1 | 18.3 |
| D078WF | Double hat | 0.78 | 30×30 | 1 | 22 |
| D078WG | Double hat | 0.78 | 30×30 | 1 | 27.5 |
| D078XF | Double hat | 0.78 | 33×27 | 1.22 | 22 |
| D078YF | Double hat | 0.78 | 36×24 | 1.5 | 22 |
| D095WF | Double hat | 0.95 | 30×30 | 1 | 22 |
| D095XF | Double hat | 0.95 | 33×27 | 1.22 | 22 |
| D095YF | Double hat | 0.95 | 36×24 | 1.5 | 22 |

**Table 2** Material constants of specimens

| Specimen Thickness [mm] | Yield Strength [MPa] | Tensile Strength [MPa] | Elongation [%] |
|---|---|---|---|
| 0.78 | 166.7 | 308.4 | 46.4 |
| 0.95 | 172.0 | 302.8 | 45.6 |

Considering the theoretical folding width of 22 mm, three types of spot weld pitch were chosen: 18.3 mm, 22 mm, and 27.5 mm.

Table 2 lists the material properties of the specimens.

### 2.2 Apparatus and method

In the impact collapse tests, the crosshead of 40 kilograms is pressed by the axial impact collapse test device using an air pressure accelerator (Cha et al., 2001). The crosshead poised by an airpressure of 0.4 MPa crashes into the specimen. The value of the impact energy is similar to that given by Eq. (1): 1034J at 7.19 m/sec.

$$E_I=\frac{1}{2}mv^2 \tag{1}$$

where $m$ is the mass of the crosshead and $v$ is the impact collapse velocity. It is considered that about 97 percent of all the impact energy is consumed to deform the specimen during the collision and about 3 percent is dissipated into repulsion energy, sliding energy, friction energy and heat.

A load-displacement curve which shows the collapse history was obtained by eliminating the time axis from the measured time-load and time-displacement curves. Based on the load-displacement curve, absorbed energy ($E_a$), mean collapse load ($P_{mean}$), maximum collapse load ($P_{max}$.) and deformed length ($S$) were derived. The absorption characteristics of each specimens were studied.

The absorbed energy is the area below the load-displacement curve, and it is calculated by integrating the load with respect to displacement, Eq. (2). The mean collapse load is obtained by dividing the absorbed energy by the displacement.

$$E_a = \int_{l_0}^{l} P dl \qquad (2)$$

where $E_a$ is the absorbed energy in the specimen and $P$ is the collapse load.

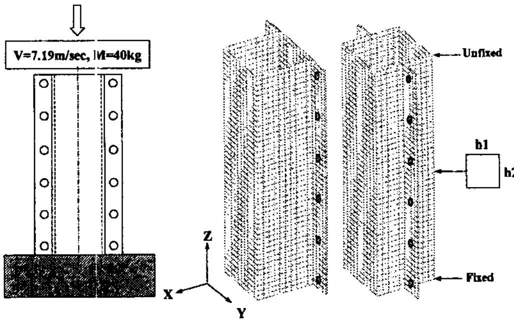


**Fig. 1** Boundary conditions in impact collapse

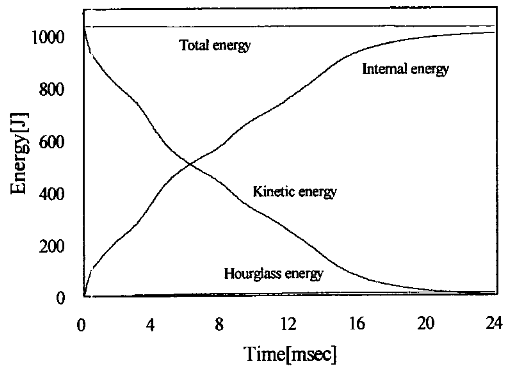


**Fig. 2** Relationship between time and energy, H078WE

## 3. Impact Collapse Simulation

In the program system presented in this study, an explicit finite element code, LS-DYNA3D (Livermore Software Technology, 1997), is adopted for simulating the complicated collapse behavior of the hat and double hat shaped section members.

Figure 1 is the finite element model used in the impact collapse simulation, with its boundary conditions. The dimensions of the model are the same as those of the experiments. The hat and double hat shaped section members are divided into Belytschko-tsay shell elements (Livermore Software Technology, 1993), four nodal shell elements of h1(3 mm)×h2( 3 mm).

Considering the conditions of the experiment (Cha et al., 2001), it has been decided that the bottom of the model is fully restrained and the top of the model is free. An arbitrary finite stone wall of mass of 40 kilograms is placed at a certain distance from the top, and strikes the top of the model at a velocity of 7.19 m/sec. The stone wall is defined as a master that strikes a slave, the nodes on the top of the specimen. The hourglass energy has been controlled to make out how it affects the total absorbed energy. As shown in Fig. 2, the hourglass energy is less than 1 percent of the total energy. This implies that the analysis is reliable.

All the material properties used in simulation are in Table 2. All shells in the model are adapted to the stress-deformation relationship in order to consider the linear and non-linear behaviors. Because of the strain rate sensitivity, the maximum collapse loads from tests are higher than the yield stress. Therefore, in this process, Eq. (3) suggested by Couper Symonds has been considered.

$$\sigma_n = \sigma_y \left( 1 + \left( \frac{\dot{\varepsilon}}{D} \right)^{1/P} \right) \qquad (3)$$

$$\dot{\varepsilon} = \sqrt{\dot{\varepsilon}_{ij} \dot{\varepsilon}_{ij}}$$

where $\sigma_y$ is the static yield stress, $\sigma_n$ is the yield

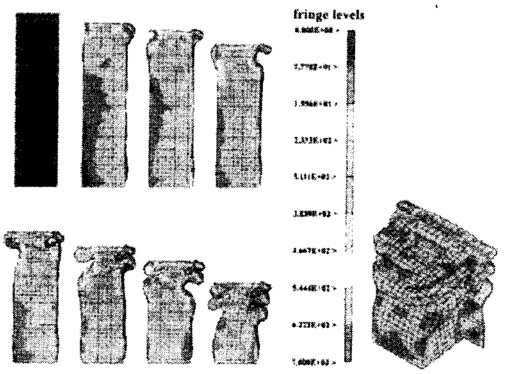


**Fig. 3** State of on Mises stress in simulation for hat-shaped member, H078WE

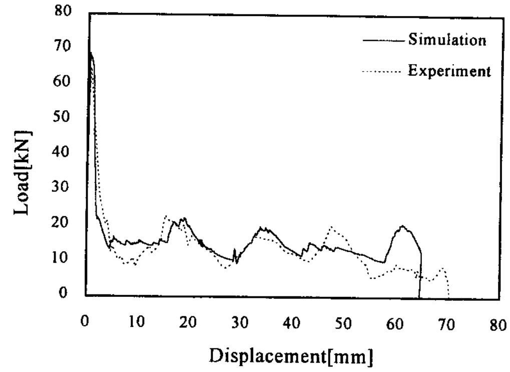


**Fig. 4** Relationship between load and displacement for hat-shaped members, H078WE

stress in high speed deformation, $\dot{\varepsilon}$ is the strain rate, and $D$ and $P$ are strain rate parameters. In this study, $D$=40.4 $s^{-1}$ and $P$=5 are used, as set by doing high speed tensile tests on SCP1 cold rolled steel (Grxebieta et al., 1986; Jonse, 1989).

In order to get the same collapse mode as in the experiment, center nodes on the top of the double hat shaped section member were moved by 0.03%. However, the imperfections on the hat shaped section members were not considered because its collapse mode was decided by the buckling of the plane which is lower than that of the ㄷ-type section.

## 4. Results and Discussion

Using the finite element method module, absorbed energy $E_a$, mean collapse loads $P_{mean}$, maximum collapse loads $P_{max.}$, and deformed length S have been arranged on the shift of section dimensions and spot weld pitches on the flange. The simulation has been verified by comparing the results with the impact collapse experiments. And the deformation mode during collapse and dynamic collapse characteristics have been analyzed, which were not available in the dynamic collapse experiments.

In Fig. 3, the stress distribution is presented while the hat shaped section member (H078WE) of thickness 0.78 mm, section dimension 30×30 mm and spot weld pitch 18.3 mm is being collapsed with an impact velocity of 7.19 m/sec. And the load-displacement curve obtained from the simulation is compared with the result from the impact collapse experiment in Fig. 4. In the same manner, Figs. 5 and 6 show the stress distribution

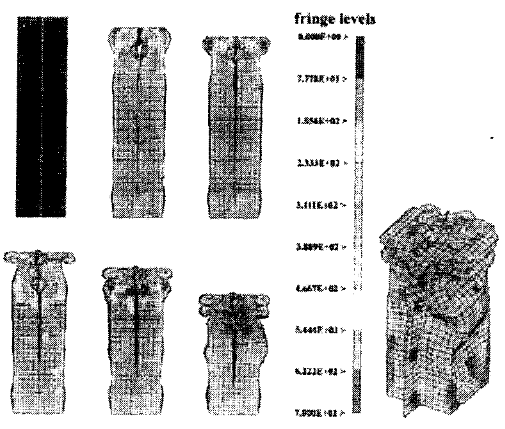


**Fig. 5** State of von Mises stress in simulation for double hat-shaped member, D078WE

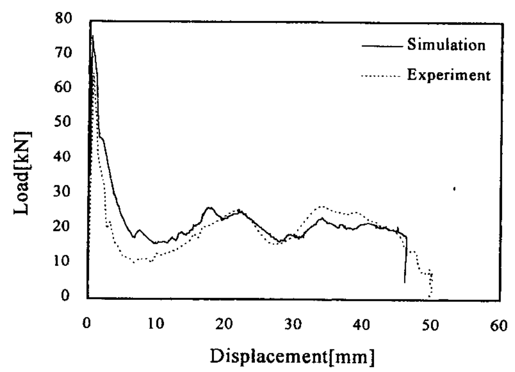


**Fig. 6** Relationship between load and displacement for double hat-shaped members, D078WE

and load-displacement relationship, respectively, for the double hat shaped section member (D078WE). The solid line shows the simulation result, and the dotted line the experimental results.

Taking a closer look into the stress distribution during collapse, after the barrier strikes the top of the model, buckling waves occur and the stress is distributed throughout the entire area in the model. And the stress is concentrated on the edges, and then buckling occurs on the plane, because the buckling stress on the edges is high. After the first fold ends, the second one occurs in the same way as the first. But the maximum collapse load of the second fold is lower than that of the first. For this reason the whole structure was plastically deformed when the barrier stroke. During the collapse, the hat shaped section member had the parallel deformation mode, in which the plane collapses toward the inside of the structure while ㄷ-shaped section member collapses toward its outside. But the double hat shaped section member has an unstable symmetrical deformation mode due to the interference of the flanges. The load and displacement curve obtained from the impact collapse experiments agrees with that obtained from simulations, and the peak loads of the simulations are slightly higher and occur faster than those of the experiments.

In Table 3, the absorbed energy, mean collapse load, maximum collapse load and deformed length in the experiment and simulation are compared with respect to variations of the section dimension. In Fig. 7, the mean collapse loads of the hat and double hat shaped section members with a thickness of 0.78 mm from the simulation and experiment are compared, and Fig. 8 shows those with a thickness of 0.95 mm. In Table 4, the absorbed energy, mean collapse load, maximum collapse load and deformed length in the experiment and simulation are compared with respect to the variations of the spot weld pitch on the flanges of hat and double hat shaped section members with a thickness of 0.78 mm. Figure 9 shows the comparison between the collapse profile from the simulation and experiment while the hat and double hat shaped section members are collapsed. Based on the results, 97 percent of the total impact energy was absorbed by the model in

**Table 3** Impact collapse test and simulation results for hat-shaped and double hat-shaped members with various section dimension

| Name. | Absorbed energy $E_a$[J] | | Mean collapse load $P_{mean}$[kN] | | | Maximum collapse load $P_{max}$[kN] | | | Deformation $S$[mm] | |
|---|---|---|---|---|---|---|---|---|---|---|
| | test $(E_a)\,t$ | simulation $(E_a)\,s$ | test $(P_{mean})\,t$ | simulation $(P_{mean})\,s$ | $(P_{mean})\,s$ / $(P_{mean})\,t$ | test $(P_{max\cdot})\,t$ | simulation $(P_{max\cdot})\,s$ | $(P_{max\cdot})\,s$ / $(P_{max\cdot})\,t$ | test $(S)\,t$ | simulation $(S)\,s$ |
| H078WF | 995.4 | 1004 | 13.1 | 13.9 | 1.06 | 61.9 | 71.4 | 1.15 | 76 | 72.2 |
| H078XF | 1005.8 | 1007 | 13.2 | 14.3 | 1.08 | 63.4 | 71.3 | 1.13 | 76 | 70.7 |
| H078YF | 1016.7 | 993 | 13.0 | 14.2 | 1.09 | 62.2 | 70.2 | 1.13 | 78 | 70.1 |
| H095WF | 1012.6 | 1003 | 19.5 | 19.7 | 1.01 | 79.7 | 85.7 | 1.07 | 52 | 51.0 |
| H095XF | 1004.0 | 999 | 17.9 | 19.7 | 1.10 | 75.7 | 83.3 | 1.10 | 56 | 50.7 |
| H095YF | 1019.1 | 1004 | 17.9 | 19.6 | 1.10 | 78.3 | 83.2 | 1.06 | 57 | 51.2 |
| D078WF | 1004.8 | 1016 | 18.6 | 19.1 | 1.03 | 68.1 | 74.3 | 1.09 | 54 | 53.2 |
| D078XF | 1013.4 | 1003 | 18.8 | 20.3 | 1.08 | 63.2 | 72.4 | 1.15 | 54 | 49.4 |
| D078YF | 981.8 | 1011 | 19.3 | 21.3 | 1.10 | 72.3 | 73.8 | 1.01 | 51 | 47.6 |
| D095WF | 996.9 | 1004 | 24.9 | 27.5 | 1.10 | 80.8 | 87.4 | 1.08 | 40 | 36.6 |
| D095XF | 985.9 | 1011 | 26.0 | 28.9 | 1.11 | 84.8 | 87.5 | 1.03 | 38 | 35.0 |
| D095YF | 989.6 | 1007 | 26.0 | 27.6 | 1.06 | 85.9 | 87.0 | 1.01 | 38 | 36.5 |

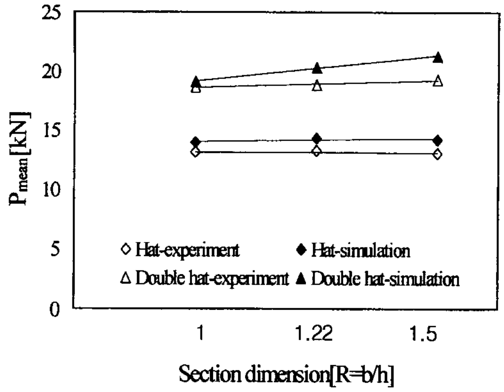


**Fig. 7** Relationship between section dimension and mean collapse load for hat-shaped and double hat-shaped members (Thickness 0.78 mm, spot-weld pitch 22 mm)

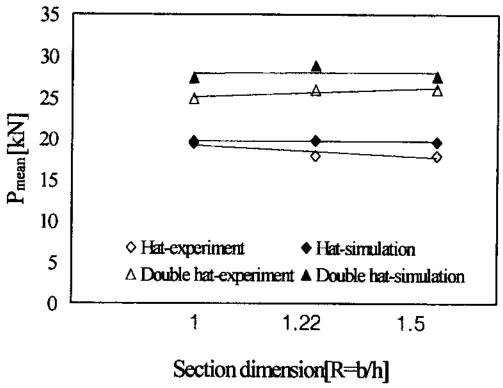


**Fig. 8** Relationship between section dimension and mean collapse load for hat-shaped and double hat-shaped members (Thickness 0.95 mm, spot-weld pitch 22 mm)

the impact collapse simulation. And it coincides with that of the impact collapse experiment, and the other 3 percent was lost in the forms of sliding interface energy, stonewall energy and hourglass energy. In Tables 3 and 4, $(E_a)\,t$ is the absorbed energy, $(P_{mean})\,t$ is the mean collapse load, $(P_{max\cdot})\,t$ is the maximum collapse load and $(S)\,t$ is deformed length from the impact collapse experiment. And $(E_a)\,s$ is the absorbed energy, $(P_{mean})\,s$ is the mean collapse energy, $(P_{max\cdot})\,s$ is the maximum collapse load and $(S)\,s$ is the deformed length from the simulation. $(P_{mean})\,s/(P_{mean})\,t$ is the ratio of the mean collapse loads, and $(P_{max\cdot})\,s/(P_{max\cdot})\,t$ is that of the maximum collapse loads.

The mean collapse load is about 10 percent higher and the maximum collapse load is about 15 percent higher than in the simulation. With respect to section dimension, there is no remarkable tendency in the impact collapse simulation similar to the experimental results. On the other hand, the mean collapse load of the hat and double hat shapedsection members increases as the spot weld pitch decreases. In consideration of the maximum collapse load, there is no correlation with the variation of the section dimension and spot weld pitch. According to the results from experiment, the mean collapse load of the double hat shaped section member is about 39 percent higher and maximum collapse load is about 6.5 percent higher than those of the hat shaped section member. In the simulation, the mean collapse load of the double hat shaped

**Table 4** Collapse test and simulation results for hat-shaped and double hat-shaped member with flange spot-weld pitch

| Name. | Absorbed energy $E_a$[J] | | Mean collapse load $P_{mean}$[kN] | | | Maximum collapse load $P_{max}$[kN] | | | Deformation $S$[mm] | |
|---|---|---|---|---|---|---|---|---|---|---|
| | test $(E_a)\,t$ | simulation $(E_a)\,s$ | test $(P_{mean})\,t$ | simulation $(P_{mean})\,s$ | $(P_{mean})\,s$ / $(P_{mean})\,t$ | test $(P_{max\cdot})\,t$ | simulation $(P_{max\cdot})\,s$ | $(P_{max\cdot})\,s$ / $(P_{max\cdot})\,t$ | test $(S)\,t$ | simulation $(S)\,s$ |
| H078WE | 1007.1 | 1005 | 14.0 | 15.5 | 1.11 | 64.8 | 68.9 | 1.06 | 72 | 64.9 |
| H078WF | 995.4 | 1004 | 13.1 | 13.9 | 1.06 | 61.9 | 71.4 | 1.15 | 76 | 72.2 |
| H078WG | 994.4 | 1007 | 12.8 | 13.8 | 1.08 | 62.5 | 68.1 | 1.09 | 78 | 73.2 |
| D078WE | 984.7 | 1014 | 19.3 | 21.9 | 1.13 | 66.1 | 75.6 | 1.14 | 51 | 46.4 |
| D078WF | 1004.8 | 1016 | 18.6 | 19.1 | 1.03 | 68.1 | 74.3 | 1.09 | 54 | 53.2 |
| D078WG | 984.6 | 1005 | 15.6 | 16.3 | 1.04 | 62.8 | 71.3 | 1.14 | 63 | 61.7 |

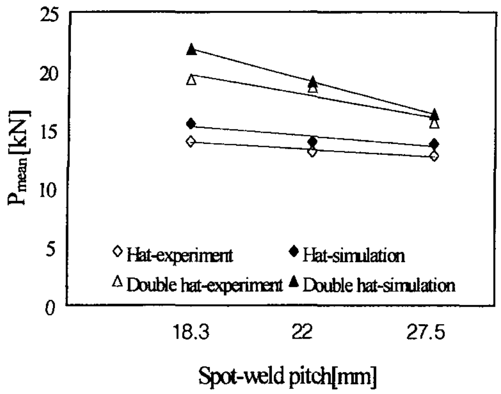


**Fig. 9** Relationship between spot weld pitch and mean collapse load for hat-shaped and double hat-shaped members (Thickness 0.78 mm, Section dimension 30×30 mm)

section member is 39.7 percent higher and the maximum collapse load is about 4.5 percent higher. In view of the results so far, the simulation generally agrees with the experiment.

## 5. Conclusions

(1) The deformation mode in the simulation is the same as in the experiments. The hat shaped section members undergo parallel deformation mode while collapsing progressively. However, most of the double hat section members undergo an unstable symmetric deformation mode due to the interference of the flanges.

(2) According to the results of both experiment and simulation, the mean collapse loads of the hat shaped section members are independent of the variation of section dimension, but those of the double hat shaped section members are higher in large section dimensions. And both hat and double hat shaped section members have excellent collapse capability, as their spot weld pitches decrease.

(3) The mean collapse loads from the impact collapse simulation are about 10 percent higher than those from the impact collapse experiment. And, the maximum collapse loads are about 15 percent higher than those in the experiment.

(4) According to the results from the experiment, the mean collapse load of the double hat shaped section member is about 39 percent higher and the maximum collapse load is about 6.5 percent higher than those of the hat shaped section members. In the simulation, the mean collapse load of the double hat shaped section member is 39.7 percent higher and the maximum collapse load is about 4.5 percent higher. It may be concluded that the results from these experiments agree with simulations, considering errors in manufacturing and testing.

## References


Cha, C. S., Kang, J. Y. and Yang, I. Y. 2001, "Axial Impact Collapse Analysis of Spot Welded Hat Shaped Section Members," *KSME International Journal*, Vol. 15, No. 2, pp. 180~191.

Grzebieta, R. H. and Murray, N. W., 1986, "Energy Absorpotion of an Initially Imperfect Strut Subjected to an Impact Load," *International Journal Impact Engineering*, Vol. 4, No. 4, pp. 147~159.

Jonse, N., 1989, Structural impact, Cambridge University Press, pp. 403~405.

Livermore Software Technology Corporation, 1993, *LS-DYNA3D Theoretical Manual*, pp. 6. 1~6. 10.

Livermore Software Technology Corporation, 1997, *LS-DYNA User's Manual*.

Santosa, S. and Wierzbicki, T., 1998, "Crash Behavior of Box Columns Filled with Aluminum Honeycomb Foam," *Computers & Structures*, pp. 333~367.

White, M. D. and Jones, N., 1999a, "Experimental Quasi-static Axial Crushing of Top-hat and Double-hat Thin-walled Sections," *International Journal of Mechanical Science*, Vol. 41, pp. 179~208.

White, M. D., Jones, N. and Abramowicz, W., 1999b, "A Theoretical Analysis for the Quasi-static Axial Crushing of Top-hat and Double-hat Thin-walled Sections," *International Journal of Mechanical Sciences*, Vol. 41, pp. 209~233.

Yamaxaki Koetsu and Han Jing, 1998, "Maximization of Crushing Energy Absorption of Tubes." *The American Institute of Aeronautics and Astronautics*, pp. 2708~2717.